Inorganic Chemistry
Article

Solid-State Structure Dependence of the Molecular Distortion and Spectroscopic Properties of the Cu(I) Bis(2,9-dimethyl-1,10-phenanthroline) Ion

Andrey Yu. Kovalevsky, Milan Gembicky, Irina V. Novozhilova, and Philip Coppens*

Chemistry Department, University at Buffalo, State University of New York, Buffalo, New York 14260

The relation between the geometry and spectroscopic properties of a series of salts of the Cu(I) bis(2,9-dimethyl-1,10-phenanthroline) ion, $(Cu^{(I)}(dmp)_2)^+$, is explored. The distortions from the idealized D_{2d} geometry, which include flattening, rocking of the dmp ligands, and displacement of the Cu atoms out of the dmp planes, show considerable variation, indicating the importance of packing forces in the crystalline environment. The change in the absorption spectra upon flattening of the complex, expressed as the variation of the angle between the dmp planes, which varies from 88° in the BF_4 and tosylate salts to 73° in the picrate, agrees qualitatively with parallel DFT calculations. No correlation is found between ground state geometry and luminescence lifetimes, recorded both at room temperature and at 16 K. The low temperature lifetimes vary by a factor of 8 among the $(Cu^{(I)}(dmp)_2)^+$ salts examined, the longest lifetime (2.4 μs at 16 K) being observed for the tosylate salt.

Introduction

A fundamental understanding of photoinduced electron transfer requires knowledge of the geometry changes accompanying the transfer process. As part of our time-resolved diffraction studies on the geometry of molecular excited states,[1] we have, as a necessary first step, examined the variation in the ground state structure and spectroscopic behavior of Cu$^{(I)}$ bisphenanthroline complexes, which undergo photoinduced metal-to-ligand charge transfer (MLCT).[2,3] They absorb light in the visible spectral region and show phosphorescence with nanosecond to microsecond scale lifetimes.

The current paper concerns the relation between the structural variation and spectroscopic changes of a series of salts of the Cu$^{(I)}$ bis(2,9-dimethyl-1,10 phenanthroline) ion, $(Cu^{(I)}(dmp)_2)^+$. This is the first time that a series of solids with an identical Cu$^{(I)}$ cation but different molecular environment has been systematically explored by both crystallographic and spectroscopic methods.

Experimental Section

Preparation of the Copper(I) Complexes. Starting Materials. CuBr, $Cu(BF_4)_2 \cdot 6H_2O$, $Cu(NO_3)_2 \cdot 6H_2O$, $[Cu(NCCH_3)_4]PF_6$, $[Cu(CNCH_3)_4]BF_4$, copper metal powder, 1,10-dimethyl-2,9-phenanthroline (dmp), tetramethylammonium tosylate (TMATos), sodium 9,10-anthraquinone-2-sulfonate (NaAQSO₃), and L-ascorbic acid are commercially available from Aldrich and were used without further purification. Tetramethylammonium calix[4]arenate (TMACalix) was synthesized by a method of Harrowfield et al.[4] Tetramethyl-ammonium picrate (TMAPic) was prepared with quantitative yield by combining a saturated solution of picric acid (Aldrich, Inc.) in water and an equimolar amount of tetramethylammonium hydroxide (25% in water) (Aldrich, Inc.). The yellow crystalline precipitate of TMAPic was filtered and dried overnight over molecular sieves.

[Cu(dmp)₂]BF₄ (1), [Cu(dmp)₂]BF₄·0.5Acetone (2), and [Cu(dmp)₂]BF₄·0.5dmp (3). The [Cu(dmp)₂]BF₄ complex was prepared by the method described previously.[5] Crystals of **1** were obtained by slow evaporation of an acetonitrile solution, while crystals of **2** were prepared by diethyl ether vapor diffusion into

* To whom correspondence should be addressed. E-mail: coppens@buffalo.edu.

(1) (a) Kim, C. D.; Pillet, S.; Wu, G.; Fullagar, W. K.; Coppens, P. *Acta Crystallogr., Sect. A* **2002**, *58*, 133–137. (b) Novozhilova, I.; Volkov, A. V.; Coppens, P. *J. Am. Chem. Soc.* **2003**, *125*, 1079–1087. (c) Coppens, P.; Novozhilova, I. *Faraday Discuss.* **2002**, *122*, 1–11. (d) Coppens, P. *Chem. Commun.* **2003**, 1317–1320. (e) Coppens, P.; Graber, T.; Vorontsov, I.; Wu, G.; Kovalevsky, A. Yu.; Gembicky, M.; Chen, Y.-S. To be published.
(2) Scaltrito, D. V.; Thompson, D. W.; O'Callaghan, J. A.; Meyer, G. J. *Coord. Chem. Rev.* **2000**, *208*, 243–266.
(3) Armaroli, N. *Chem. Soc. Rev.* **2001**, *30*, 113–124.
(4) Harrowfield, J. M.; Ogden, M. I.; Richmond, W. R.; Skelton, B. W.; White, A. H. *J. Chem. Soc., Perkin Trans.* **1993**, *2*, 2183–2190.
(5) McMillin, D. R.; Buckner, M. T.; Ahn, B. T. *Inorg. Chem.* **1977**, *16*, 943–945.

an acetone solution of the copper complex. Product **3** in which unligated dmp cocrystalizes with the complex was obtained by slow evaporation of an acetonitrile/water (2:1 v/v) solution containing the copper compound and an equimolar amount of free dmp ligand. Every procedure described here and below gave crystals suitable for X-ray diffraction analysis.

[Cu(dmp)₂]PF₆ (4) and [Cu(dmp)₂]PF₆·0.5CH₂Cl₂ (5). [Cu(dmp)₂]PF₆ was synthesized by a known procedure.[5] Crystals of **4** were prepared by slow evaporation of an acetonitrile/water (2:1 v/v) solution, while crystals of **5** were grown by diethyl ether vapor diffusion into a solution of the complex in dichloromethane.

[Cu(dmp)₂]NO₃·2H₂O (6). Cu metal powder was added to a green acetonitrile solution containing $Cu(NO_3)_2 \cdot 6H_2O$ and dmp (4-fold excess) in order to reduce Cu(II) to Cu(I). The resulting mixture was suspended in an ultrasonic bath for 15 min. After the insoluble residue was removed by filtration, the clear red solution was slowly evaporated to give a crystalline product (∼90% yield). Compound **6** can also be prepared by the same procedure but with L-ascorbic acid replacing copper metal powder as a reducing agent.

[Cu(dmp)₂]Calix (7). An acetonitrile solution of CuBr and a stoichiometric amount of dmp were refluxed for 2 h. To the resulting red clear solution was added TMACalix (10% excess in acetonitrile) and the mixture left to slowly evaporate over a period of several days. Well-formed crystals of the product were collected by filtration and dried in air to give an 80% yield.

[Cu(dmp)₂]Tos (8). [Cu(NCCH₃)₄]BF₄ and a stoichiometric amount of dmp were dissolved in an acetonitrile/water mixture (2:1 v/v). TMATos (10% excess) was added to the resulting solution which was refluxed for 2 h. Slow evaporation of the solution gave good crystals of the product in 70% yield.

[Cu(dmp)₂]AQSO₃·CH₃CN (9) and [Cu(dmp)₂]AQSO₃·0.5H₂O (10). Stoichiometric amounts of NaAQSO₃ and $Cu(BF_4)_2 \cdot 6H_2O$ were dissolved in water (50 mL) at 70 °C. To the clear solution was added a stoichiometric amount of dmp dissolved in ethanol. A greenish precipitate was formed immediately. Ascorbic acid was added to the suspension to reduce Cu(II) to Cu(I). The color of the precipitate changed to orange. The resulting suspension was stirred for an additional 2 h at 70 °C and cooled to room temperature. The orange solid was filtered, washed with diethyl ether, and dried in air to give 86% of [Cu(dmp)₂]AQSO₃. Crystals of **9** (large orange-red prisms) were grown by diethyl ether vapor diffusion into an acetonitrile solution of the product. Crystals of **10** (orange plates) were obtained by the same method using an acetone solution.

[Cu(dmp)₂]Pic (11). Complex **11** was prepared in quantitative yield in a similar way as **8**, with the exception that TMATos was replaced by TMAPic. The crystals were obtained by a slow evaporation of the reaction mixture.

X-ray Crystallography. X-ray diffraction data on **1**−**11** were collected at 90(1) K using a Bruker SMART1000 CCD diffractometer installed at a rotating anode source (Mo Kα radiation) and equipped with an Oxford Cryosystems nitrogen gas-flow apparatus. The data were collected by the rotation method with 0.3° frame width (ω scan) and 20−40 s exposure time per frame. For each complex, four data sets (600 frames in each set) were collected, nominally covering half of reciprocal space. The data were integrated, scaled, sorted, and averaged using the SMART software package.[6] The structures were solved by direct methods, using SHELXTL NT version 5.10,[7] and refined by full-matrix least-

squares against F^2. The displacement parameters of non-hydrogen atoms were refined anisotropically. Hydrogen atoms were located in difference electron density maps and subsequently refined using the riding model for aromatic and methylene H atoms with $U_{iso} = 1.2U_{eq}$ of the connected carbon, and in idealized positions for CH₃, OH, and H₂O with $U_{iso} = 1.5U_{eq}$.

Acetone and dichloromethane solvent molecules in **2** and **5**, respectively, are disordered into two equally occupied positions through inversion centers. In **3** the nonligated dmp molecule and the acetonitrile solvent molecule included in the crystal occupy the same crystallographic site with 50%/50% population. In addition, two of the four fluorine atoms of the BF_4^- counterion are disordered over two equally populated positions. The atoms of the disordered molecules were refined isotropically. The picrate counterion in **11** is disordered by 120° rotations around the local pseudo-3-fold axis perpendicular to its central benzene ring. The oxygen atom of the picrate ion occupies three positions with 70%/20%/10% population and was refined isotropically.

No phase transitions were observed for any of the crystals studied upon cooling from room temperature to 90 K.

UV−Vis Absorption and Photoluminescence Spectroscopy. UV−vis absorption experiments were performed on a Perkin-Elmer Lambda 35 UV−vis spectrometer equipped with an integrating sphere for reflectance spectroscopy. The spectra were collected in the 300−1100 nm range at room temperature from freshly drybox prepared KBr pellets. Photoluminescence measurements were carried out on a home-assembled emission detection system. Samples (∼0.5−1 mm-sized single crystals, except for compound **10**, for which several small single crystals were used) were mounted on a copper pin attached to a DISPLEX cryorefrigerator. A metallic vacuum chamber with quartz windows is attached to the cryostat, and the chamber is evacuated to approximately 10^{-7} bar with a turbo-molecular pump. Samples can be cooled to 15−16 K. The crystals were irradiated with 365 nm and/or 500 nm light from a pulsed N₂-dye laser. The emitted light was collected by an Oriel 77348 PMT device, positioned at 90° to the incident laser beam, and processed by a DSO-2102S computer-based digital oscilloscope with 100 MHz sampling rate.

Theoretical Calculations. Calculations were carried out with the ADF2002 suite of programs.[8] The VWN and B88LYP functionals were used in the local density approximation (LDA) and the general gradient approximation (GGA), respectively. The atomic orbitals of copper were described by a triple-ζ Slater-type basis set (ADF database TZP), while for the carbon, nitrogen, and hydrogen atoms a double-ζ Slater-type basis sets with one polarization function (ADF database DZP) was used. The (1s2s2p)[10] core shell of Cu and (1s)² core shell of C and N were treated by the frozen-core approximation. Relativistic effects were taken into account using the "zeroth order regular approximation" (ZORA). Geometry optimization was performed in the D_2 point group. The geometry was converged to the threshold of 10^{-4} Hartree/Å on the Cartesian gradients. The integrals were evaluated numerically with an accuracy of 8 significant digits. Time-dependent density functional theory (TD-DFT) calculations were carried out with the same functional used in the geometry optimization.

(6) *SMART and SAINTPLUS−Area Detector Control and Integration Software,* version 6.01; Bruker AXS: Madison, WI, 1999.

(7) *SHELXTL−An Integrated System for Solving, Refining and Displaying Crystal Structures from Diffraction Data*, version 5.10; Bruker AXS: Madison, WI, 1997.

(8) te Velde, G.; Bickelhaupt, F. M.; van Gisbergen, S. J. A.; Fonseca Guerra, C.; Baerends, E. J.; Snijders, J. G.; Ziegler, T. *J. Comput. Chem.* **2001**, *22*, 931−967.

(9) Blaskie, M. W.; McMillin, D. R. *Inorg. Chem.* **1980**, *19*, 3519−3522.

(10) Scaltrito, D. V.; Thompson, D. W.; O'Callaghan, J. A.; Meyer, G. J. *Coord. Chem. Rev.* **2000**, *208*, 243−266.

Results and Discussion

Structures of the Cu(dmp)$_2^+$ ion in Different Solids. Crystallographic and selected structural data for complexes **1**−**11** are given in Tables 1 and 2, respectively. Final positional, isotropic, and anisotropic displacement parameters together with full list of bond lengths and angles are listed in the Tables S1−S44 of the Supporting Information.

Since the first synthesis of Cu(dmp)$_2^+$ by McMillin et al.[5] in 1977 and the discovery[9] that it is photoluminescent at room temperature in solution, a great amount of effort has been invested in the exploration of the photochemistry and photophysics of this and related systems.[10] However, the reported Cu(dmp)$_2^+$ structures are limited to room temperature determinations,[11] and a detailed study of the effect of the packing in the crystal on the cation's geometry and spectroscopic behavior is lacking.

In the solids studied, the copper cation adopts a variety of conformations with various degrees of rocking and flattening distortions. A recent calculation shows the frequencies of the normal modes corresponding to these distortions to be only about 20 cm^{-1}; thus, they can easily be induced by relatively weak intermolecular forces.[12]

rocking   flattening

The rocking distorts the molecules from a close-to-tetrahedral to a trigonal pyramidal geometry. This results in one of the Cu−N bonds moving to the axial position of the trigonal pyramid, and consequently becoming longer than the other three bonds. The flattening, on the other hand, distorts the molecules toward the square planar geometry. Following White and co-workers,[11b] these distortions can be described by the three angles θ_x, θ_y and θ_z, where the first two θ's describe the rocking distortions and the third θ_z describes the flattening (Figure 1). The perfect tetrahedral geometry is illustrated by the three angles being 90°. In the case of the trigonal pyramidal geometry, θ_x or θ_y is 0°, while θ_z remains 90°. When the Cu$^{(I)}$ system is square planar, θ_x and θ_y values reach 90°, while θ_z decreases to 0°.

The distortions of complexes **1**−**11** are compared in Table 2. In the complexes studied, the θ angles range from 78.2° to 89.8° for θ_x, from 74.0° to 86° for θ_y, and from 72.8° to 88.1° for θ_z. Three distinct types of Cu(dmp)$_2^+$ geometries can be distinguished (Table 2).

(11) (a) Hoffman, S. K.; Corvan, P. J.; Singh, P.; Sethulekshmi, C. N.; Metzger, R. M.; Hatfield, W. E. *J. Am. Chem. Soc.* **1983**, *105*, 4608−4617. (b) Dobson, J. F.; Green, B. E.; Healy, P. C.; Kennard, C. H. L.; Pakawatchai, C.; White, A. H. *Aust. J. Chem.* **1984**, *37*, 649−659. (c) Dessy, G.; Fares, V. *Cryst. Struct. Commun.* **1979**, *8*, 507−510. (d) Kon, A. Yu.; Burshtein, I. F.; Proskina, N. N.; Ibragimov, B. T. *Koord. Khim.* **1987**, *13*, 260−263. (e) Hamalainen, R.; Ahlgren, M.; Turpeinen, U.; Raikas, T. *Cryst. Struct. Commun.* **1979**, *8*, 75−80. (f) Hamalainen, R.; Turpeinen, U.; Ahlgren, M.; Raikas, T. *Finn. Chem. Lett.* **1978**, 199−202. (g) Blake, A. J.; Hill, S. J.; Hubberstey, P.; Li, W.-S. *J. Chem. Soc., Dalton Trans.* **1998**, 909−916.
(12) Zgierski, M. Z. *J. Chem. Phys.* **2003**, *118*, 4045−4051.

Type 1 occurs in compounds **6**, **8**, and **9** and is described by slight distortions around the copper center, with θ angles ranging from 87.1° to 89.7° for θ_x, 84.3° to 86° for θ_y, and 84.8° to 88.1° for θ_z.

Type 2 occurs in compounds **1**, **2**, **3**, and **10** (the second of the two independent molecules) and is manifested by the rocking being more pronounced than the flattening distortion, the θ angles being 78.2−89.8° for θ_x, 74.0−81.5° for θ_y, and 81.5−88.1° for θ_z.

Type 3 occurs in compounds **4**, **5**, **7**, **10** (the first molecule), and **11**, and is characterized by the flattening being equal to or more pronounced than the rocking distortion, the θ angles ranging from 80.2° to 88.8° for θ_x, 74.4° to 85.4° for θ_y, and 72.8° to 81.9° for θ_z.

While flattening-only lowers the molecular symmetry from D_{2d} to D_2, and rocking-only leads to C_s symmetry, in all cases both distortions occur to some extent, so that the actual symmetry is lowered to C_1.

The least distorted geometry of the Cu(dmp)$_2^+$ cation is found in the tosylate complex **8**, which shows rocking and flattening of only 4° and 2°, respectively. The highest degree of rocking distortion takes place in the tetrafluoroborate acetone semisolvate compound **2**, with a θ_y value of 74.0°, while the most flattened copper(I) cation is that of the picrate salt, the dmp planes being rotated with respect to each other by almost 17° with θ_z equaling 72.8° (Figure 2). Although the nitrate dihydrate complex **6** has a very insignificantly distorted Cu$^{(I)}$ cation, it is 22.6° flattened ($\theta_z = 67.4°$) in the case of a similar nonhydrated compound reported by Hamalainen and co-workers.[11e]

It is worth noting that the copper atom is displaced from one or both of the phenanthroline planes in all the complexes (Table 2), and that this displacement is correlated with the extent of the rocking distortion: the larger the rocking, the more the copper is displaced. In complex **2**, which exhibits the largest rocking distortion, the copper atom is displaced by 0.442 Å from the plane of one of the coordinated dmp ligands. Flattening on the other hand does not produce such large copper displacements. An additional correlation exists between the rocking distortion and the lengthening of one of the Cu−N bond distances. As one of the Cu−N bonds gets closer to the axial position of the trigonal pyramid, it becomes longer than the other three bonds in pseudoequatorial positions.

The Cu(dmp)$_2^+$ cations form π−π dimers in the majority of the crystals studied. The exceptions are **1**, **7**, and **9**, in which the packing is such that the dmp ligands do not interact with each other. The π−π stacking modes are schematically illustrated in Figure 3. In **3**, the dimers are interconnected by the cocrystallized free dmp molecules, forming stacks interrupted randomly by the included acetonitrile solvent molecules. The distances between the π−π interacting dmp planes in these dimers are in the range 3.30−3.60 Å. The closest contact occurs in a dimer of complex **11**, the distance being 3.30 Å, although the dmp ligands involved do not overlap much, as shown in Figure 3. The largest plane-to-

Table 1. Crystallographic Data for Cu(dmp)$_2$$^+$ Complexes

	BF$_4$ **1**	BF$_4$·0.5Acetone **2**	BF$_4$·0.5DMP· 0.5CH$_3$CN **3**	PF$_6$ **4**	PF$_6$· 0.5CH$_2$Cl$_2$ **5**	NO$_3$·2H$_2$O **6**	calix[4]- arenate **7**	p-Tos **8**	AQSO$_3$· CH$_3$CN (α-form) **9**	AQSO$_3$· 0.5H$_2$O (β-form) **10**	picrate·CH$_3$CN **11**
empirical formula	CuC$_{28}$H$_{32}$-N$_4$BF$_4$	CuC$_{29.5}$H$_{27}$-BF$_4$N$_4$O$_{0.5}$	CuC$_{36}$H$_{31.5}$-BF$_4$N$_{5.5}$	CuC$_{28}$H$_{24}$-F$_6$N$_4$P	CuC$_{28.5}$H$_{25}$-ClF$_6$N$_4$P	CuC$_{28}$H$_{28}$-N$_5$O$_5$	CuC$_{56}$H$_{47}$-N$_4$O$_4$	CuC$_{35}$H$_{31}$-N$_4$O$_3$S	CuC$_{44}$H$_{34}$-N$_5$O$_5$S	CuC$_{42}$H$_{32}$-N$_4$O$_{5.5}$S	CuC$_{36}$H$_{29}$-N$_8$O$_7$
cryst size (mm^3)	0.2 × 0.2 × 0.15	0.1 × 0.1 × 0.05	0.45 × 0.13 × 0.10	0.2 × 0.15 × 0.13	0.2 × 0.13 × 0.1	0.2 × 0.13 × 0.05	0.3 × 0.08 × 0.08	0.25 × 0.15 × 0.15	0.25 × 0.15 × 0.15	0.50 × 0.22 × 0.03	0.40 × 0.10 × 0.10
cryst syst	orthorhombic	triclinic	triclinic	monoclinic	triclinic	triclinic	monoclinic	monoclinic	triclinic	triclinic	triclinic
space group	P2$_1$2$_1$2$_1$	P1̄	P1̄	P2$_1$/n	P1̄	P1̄	P2$_1$/c	P2$_1$/n	P1̄	P1̄	P1̄
a (Å)	11.7315(2)	10.6290(2)	10.6765(3)	13.2144(4)	10.5250(3)	7.4323(2)	8.8004(1)	12.6875(4)	7.8186(9)	13.6845(8)	7.2387(1)
b (Å)	12.0990(2)	11.0188(2)	11.3008(4)	10.7139(3)	11.1161(3)	11.8200(3)	23.2875(3)	12.1294(4)	12.116(3)	14.3426(9)	15.2434(2)
c (Å)	18.0211(2)	12.8262(2)	13.4806(4)	18.4938(5)	13.3764(3)	15.4847 (4)	21.1354(3)	19.6593(7)	19.396(3)	18.5853(11)	15.9167(2)
α (deg)	90.00	67.681(1)	96.747(1)	90.00	69.721(1)	71.243(1)	90.00	90.00	89.329(8)	89.070(3)	107.289(1)
β (deg)	90.00	73.716(1)	90.082(1)	92.449(1)	72.974(1)	82.344(1)	101.831(1)	100.835(1)	83.548(5)	71.368(2)	101.164(1)
γ (deg)	90.00	73.036(1)	107.419(1)	90.00	72.455(1)	86.619(1)	90.00	90.00	87.847(7)	78.308(2)	97.172(1)
V (Å^3)	2557.90(7)	1304.54(4)	1539.99(8)	2615.9(1)	1368.32(6)	1276.41(6)	4239.46(9)	2971.4(2)	1824.4(5)	3380.2(4)	1613.71(4)
Z	4	2	2	4	2	2	4	4	2	4	2
ρ$_{calcd}$, cm^{-3}	1.472	1.517	1.491	1.587	1.620	1.504	1.416	1.456	1.472	1.525	1.542
θ max	30.01	30.52	28.32	27.00	28.30	30.03	26.37	31.06	30.14	25.06	28.30
reflns collected	45136	24826	30723	38846	25516	22246	44443	56035	32584	21583	34542
unique reflns (R$_{int}$)	7462 (0.041)	7980 (0.052)	7618 (0.036)	5702 (0.045)	6704 (0.035)	7106 (0.046)	8645 (0.045)	9496 (0.044)	10607 (0.026)	11755 (0.032)	7991 (0.033)
obsd reflns (no. params)	6898 (347)	6490 (375)	6589 (400)	4452 (365)	5710 (384)	5467(356)	7001 (590)	7658 (403)	9690 (511)	8963 (972)	6976 (478)
R1 (F > 4(σ)F), wR2	0.027, 0.070	0.039, 0.105	0.053, 0.152	0.039, 0.106	0.034, 0.090	0.039, 0.098	0.037, 0.101	0.033, 0.087	0.029, 0.084	0.037, 0.095	0.036, 0.096
GOF	1.111	1.071	1.167	1.026	1.070	1.050	1.079	1.056	1.047	1.027	1.082

Table 2. Selected Structural Data for Cu(dmp)$_2^+$ Complexes (distances in Å)

	BF$_4$ 1	BF$_4$·0.5AC 2	BF$_4$·0.5DMP 3	PF$_6$ 4	PF$_6$· 0.5CH$_2$Cl$_2$ 5	NO$_3$·2H$_2$O 6	calix[4]- arene 7	p-TOS 8	α-AQSO$_3$· CH$_3$CN 9	β-AQSO$_3$· 0.H$_2$O 10	picrate 11
Cu–N1A	1.997(1)	2.000(1)	2.022(2)	2.028(2)	2.008(2)	2.024(2)	2.018(2)	2.013(1)	2.016(1)	2.022(2), 1.990(2)	2.026(1)
Cu–N2A	2.014(1)	2.043(1)	2.036(2)	2.042(2)	2.046(2)	2.031(2)	2.032(2)	2.014(1)	2.030(1)	2.045(2), 2.013(2)	2.030(1)
Cu–N1B	2.023(1)	2.047(2)	2.054(2)	2.053(2)	2.054(2)	2.033(2)	2.035(2)	2.015(1)	2.031(1)	2.050(2), 2.047(2)	2.037(1)
Cu–N2B	2.045(1)	2.112(2)	2.074(2)	2.070(2)	2.116(2)	2.039(2)	2.053(2)	2.021(1)	2.062(1)	2.076(2), 2.086(2)	2.043(1)
N1–Cu–N2(deg)	82.86(5)	81.69(6)	82.05(9)	81.78(8)	81.70(6)	82.64(6)	82.37(7)	82.93(5)	82.41(4)	81.60(8), 81.78(9)	82.66(6)
N3–Cu–N4(deg)	83.05(5)	81.77(6)	82.15(9)	81.95(8)	81.78(6)	83.10(6)	82.67(7)	82.97(5)	82.92(4)	81.76(8), 82.54(9)	82.89(6)
N1–Cu–N1(deg)	115.42(5)	109.85(6)	116.08(10)	110.75(8)	103.27(6)	118.62(6)	111.75(7)	120.84(5)	117.78(4)	113.62(8), 108.24(8)	111.68(6)
N1–Cu–N2(deg)	119.23(5)	119.28(6)	122.59(9)	126.67(8)	124.24(6)	122.72(6)	125.19(7)	122.52(5)	123.79(4)	122.00(8), 121.65(8)	119.68(6)
N2–Cu–N1(deg)	129.68(5)	129.38(6)	126.66(9)	128.42(8)	133.07(6)	123.83(6)	127.47(7)	125.22(5)	127.12(4)	126.85(8), 123.64(9)	131.68(6)
N2–Cu–N2(deg)	130.48(5)	137.44(6)	132.41(10)	132.11(8)	134.26(6)	131.28(6)	132.91(7)	127.81(5)	128.01(4)	135.65(8), 139.74(9)	135.49(6)
θ_x(deg)	88.0	89.0	89.8	86.1	80.2	88.2	87.7	89.7	87.1	88.8, 78.2	87.8
θ_y(deg)	79.6	74.0	81.5	80.1	74.4	84.3	81.9	86.0	84.4	78.8, 75.9	85.4
θ_z(deg)	88.1	81.5	84.1	79.4	76.1	84.8	78.2	88.1	87.2	81.9, 87.0	72.8
Cu displacement from dmp plane (Å)	0.007	0.021	0.021	0.095	0.090	0.033	0.028	0.114	0.026	0.036, 0.054	0.003
	0.176	0.442	0.263	0.246	0.364	0.052	0.096	0.115	0.217	0.235, 0.386	0.099
closest contact (atom, distance)	F 5.98	F 4.72	F 4.87	F 4.25	F 4.74	O 5.32	O 6.98	O 6.84	O2 4.43	Cu1–O8 4.43, Cu1–O6 4.60, Cu2–O1 4.42, Cu2–O3 4.33	N1 s 4.81
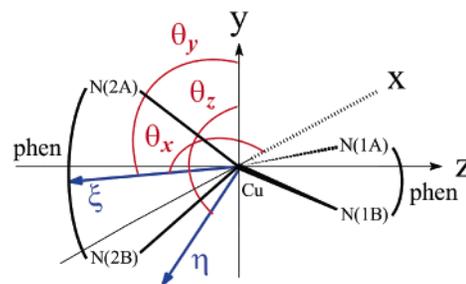
Figure 1. Schematic representation of the distortions around the copper center in Cu$^{(I)}$(dmp)$_2^+$ complexes. The θ_x and θ_y angles describe the rocking distortion, and θ_z the flattening distortion. The coordinate system is chosen so that triangle N1A–Cu–N1B lies in the XZ plane. Unit vector ξ bisects angle N2A–Cu–N2B, and unit vector η is perpendicular to triangle N2A–Cu–N2B. θ_x is the angle between ξ and X. θ_y is the angle between ξ and Y. θ_z is the angle between η and Y.

plane separation (3.60 Å) is within dimers in the PF$_6$ complexes **4** and **5**. In **4**, but not in **5**, the dmp ligands overlap strongly.

In the crystal of **11** containing the flat picrate (Pic) counterion, no $\pi-\pi$ interactions are present between the dmp ligands and the picrate anions. Instead, the Pic$^-$ anions form infinite stacks, with plane-to-plane distances of 3.39 and 3.32 Å. A completely different packing is found in the crystals **9** and **10**, in which the counterion is electron accepting 9,10-anthraquinone-2-sulfonate (AQSO$_3$) (Figure 4). In **9**, one dmp ligand and the anion form infinite alternating stacks (Figure 4a), with a minimum separation of 3.30 Å and almost parallel dmp and AQSO$_3$ planes. The N$_{dmp}$–O$_{AQSO3}$ contact is 3.5 Å, and close interactions O2···C4′ ($x + 1, y, z$) 3.31 Å and O2···C5′ 3.19 Å exist with the other dmp ligand. In **10**, which contains two independent molecules, AQSO$_3^-$ anions form a larger number of contacts with the dmp ligands, although with less overlapping of the ring systems. The closest contacts are O1···N6 3.62 Å, C67···C1′ ($x + 2, y + 1, z$) 3.31 Å (Figure 4b), and O6···N2″ ($1 - x, y, z$) 3.75 Å, C80···C31‴ ($x + 1, y + 2, z + 1$) 3.43 Å, C81···C30‴ 3.30 Å (Figure 4c). In addition, two of the dmp ligands interact with a plane-to-plane separation of 3.50 Å.

UV–Vis Absorption. UV–vis absorption (reflectance) and photoluminescence measurements were performed on crystalline samples of all 11 Cu(dmp)$_2^+$ complexes. The reflectance spectra are similar in the visible region, although there are differences in detail (Table 3).

The idealized ground state geometry of the Cu(dmp)$_2^+$ complexes corresponds to a pseudotetrahedral arrangement of phenanthroline ligands around the copper center with D_{2d} symmetry. According to Parker and Crosby[13] and more recent calculations,[12,14] in D_{2d} symmetry four low-energy singlet–singlet transitions from the degenerate highest occupied orbital of E symmetry to the lowest unoccupied orbitals (e$_{xz,yz}$ → e$_{dmp}$, with z along the principal 2-fold axis, x and y along the other 2-fold axes) are possible. Only one of these transitions has its dipole moment operator along the 2-fold axis and is therefore symmetry-allowed in D_{2d}. Thus, in solution the absorption spectrum of Cu(dmp)$_2^+$ contains only

(13) Parker, W. L.; Crosby, G. A. *J. Phys. Chem.* **1989**, *93*, 5692–5696.
(14) Novozhilova, I.; Coppens, P. To be published.

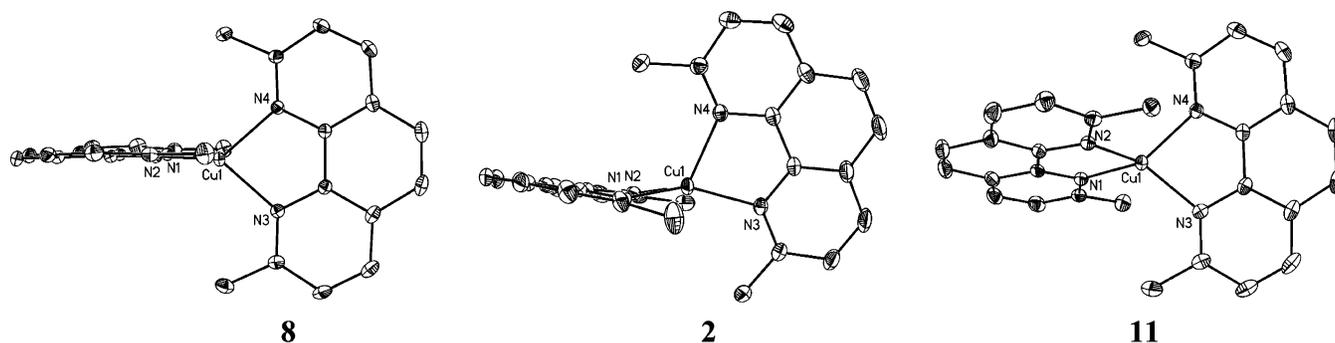**Figure 2.** Geometries of Cu(dmp)$_2^+$ cation in the complexes **2** (tetrafluoroborate acetone), **8** (tosylate), and **11** (picrate). The complexes are drawn in the plane containing the N$_3$−C−C−N$_4$ atoms.
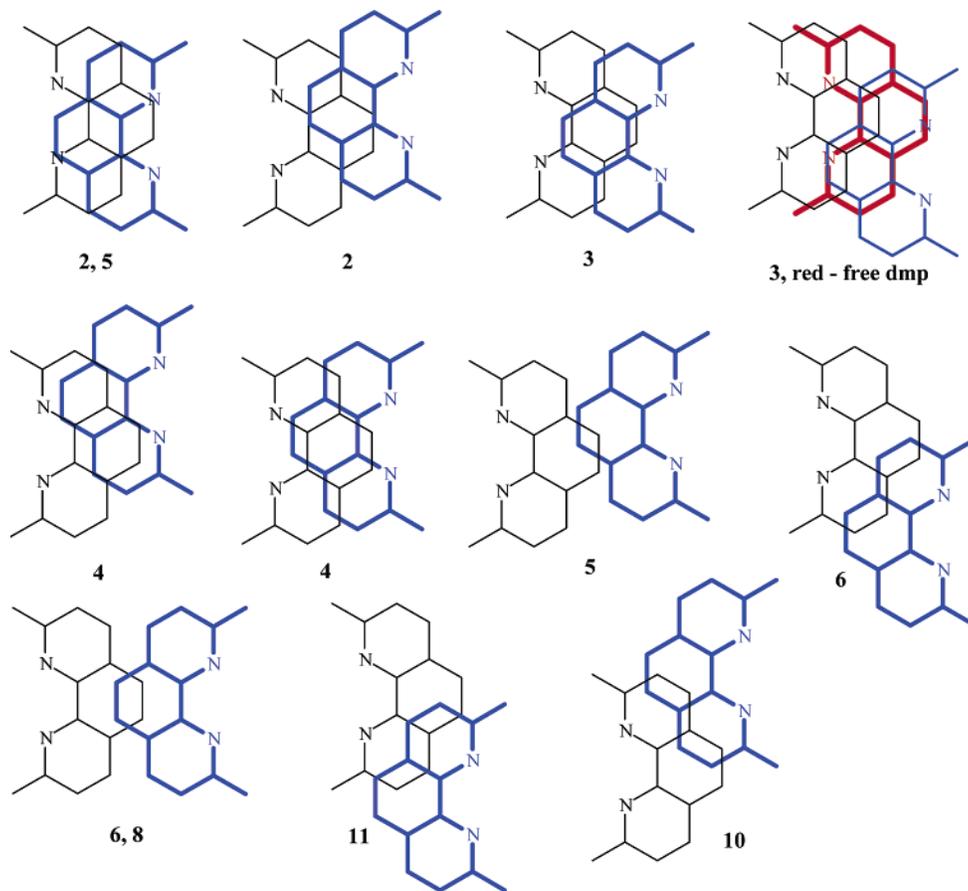

Figure 3. The schematic representation of the $\pi-\pi$ stacking modes of the dmp ligands in the crystals of **2**−**6**, **8**, **10**, and **11**. The free cocrystallized dmp molecule of complex **3** is in red.

one visible absorption band around 450 nm. However, in the solid state, symmetry-lowering to point group C_1 resulting from the geometric distortions lifts the symmetry selection rules. As a result, the MLCT transition in the solid state spectra gives rise to two bands which occur around 450 and 550 nm.[15]

As reported by Karpishin et al.,[16] small 5−15° deviations of the θ angles are sufficient for the appearance of the red-shifted second band. This is confirmed by the reflectance spectra of complexes **1**−**10**, which show two low-energy

absorption bands centered at 422−465 and 564−588 nm. For the picrate salt **11** which displays the highest degree of the ground-state flattening distortion ($\theta_z = 72.8°$, Table 2), the second band is further red-shifted to 622 nm, while the first band blue shifts to the extent that it becomes a shoulder at the 425 nm band (Table 3). These shifts result in the color of **11** being almost purple, compared to the orange-red color of the other complexes. Similar shifts of the absorption bands have been reported for other complexes with large flattening distortion.[17]

The two MLCT absorption bands of type 1 complexes are at 451−465 and 570−585 nm and are significantly red- and

(15) Felder, D. F.; Nierengarten, J.-F.; Barigelletti, F.; Ventura, B.; Armaroli, N. *J. Am. Chem. Soc.* **2001**, *123*, 6291−6299.
(16) Miller, M. T.; Gantzel, P. K.; Karpishin, T. B. *Inorg. Chem.* **1999**, *38*, 3414−3422.

(17) Cunningham, C. T.; Moore, J. J.; Cunningham, K. L. H.; Fanwick, P. E.; McMillin, D. R. *Inorg. Chem.* **2000**, *39*, 3638−3644.
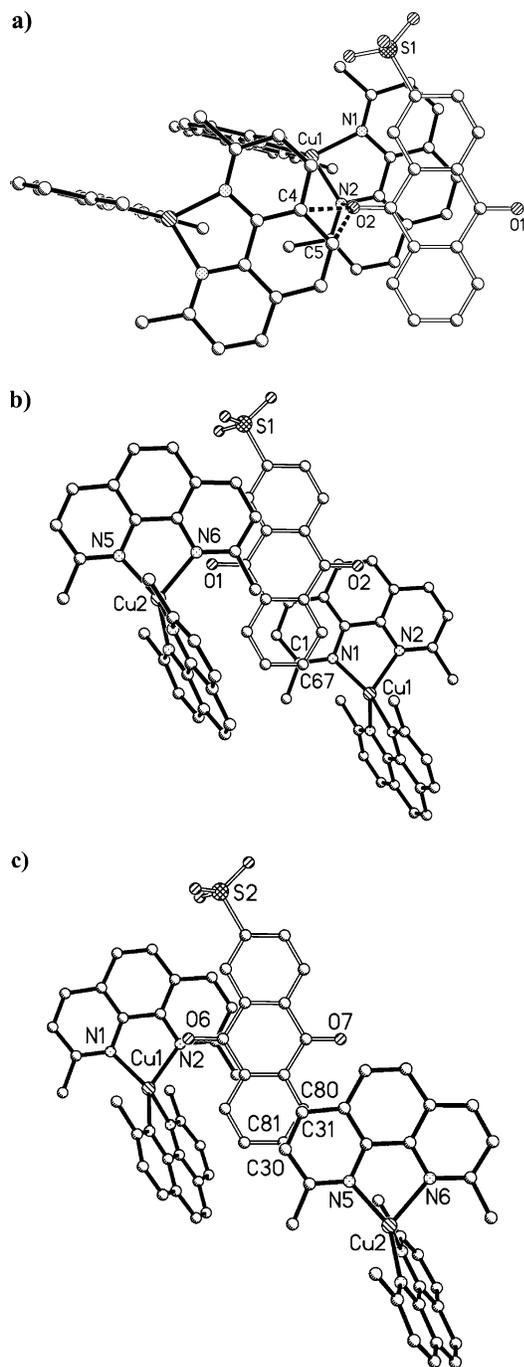
Figure 4. Stacking interactions between AQSO$_3$ anions and Cu(dmp)$_2^+$ cations in complexes **9** (a) and **10** (b, c). AQSO$_3^-$ is sandwiched between dmp ligands.

blue-shifted, respectively, relative to the similar bands of complex **11**. The positions of the absorption bands of type 2 complexes **1**, **2**, and **3** fall in an almost identical range of 455−460 and 564−588 nm. In the case of compound **10**, which has two independent and differently distorted molecules in its asymmetric unit, the spectrum is the same as that measured for the type 1 and 2 systems, the bands being centered at 454 and 585 nm. In contrast, the higher-energy bands in greatly flattened type 3 complexes **4**, **5**, and **7** are blue-shifted and appear at 422−445 nm, similar to the shift observed for the picrate complex. However, the lower-energy bands remain at 564−575 nm as in the other compounds.

In summary, when the flattening distortion occurs without any significant rocking, the lower-energy band red-shifts considerably, corresponding to the HOMO−LUMO gap being decreased, and the higher-energy band blue-shifts. Our DFT calculations of the orbital energies of Cu(I)(dmp)$_2^+$ ion at different levels of flattening (Figure 5) indicate increasing splitting of the d$_{xz}$, d$_{yz}$ HOMO upon distortion from D_{2d} to D_2 symmetry (Figure 5a). The energies of the absorption bands calculated with TD-DFT show the effect of the increased splitting and are in agreement with the observed shift upon flattening (Figure 5b).

The ∼450 nm band also moves to higher energy in the complexes with large and virtually equal rocking and flattening distortions; however, the lower-energy band does not change, as in the compounds with very small distortions. Interestingly, the rocking distortion alone or in combination with small-to-moderate flattening distortion (4−8°) does not change the absorption spectrum, which is practically the same as for the undistorted systems. For the solids studied here, the distortions (especially flattening) have to be more than 10° in order to have a pronounced effect on the UV−vis absorption spectrum.

The absorption bands in the UV region observed at 330−340 nm are assigned to the ($\pi-\pi^*$) transitions centered on the dmp ligands,[18] a conclusion supported by our calculations. The near-UV bands appearing for all the complexes, except **11**, at 403−428 nm are due to the d$_{xy}$ → π^*_{dmp} transition, which does not shift upon distortion of the cation (Figure 5b).

Emission Spectra and Lifetimes. In the crystalline state, complexes **1**−**9** and **11** show weak red photoluminescence. The emission is characterized by the broad featureless spectra with the maxima positioned in the 660−720 and 690−760 nm range at room and low (16 K) temperatures, respectively (Table 3).

It has been observed before that the luminescence intensity decreases with lowering the temperature, but the excited state lifetime increases. This behavior has been explained by McMillin and co-workers[19] on the assumption that the emission originates from two different excited states, a singlet and a triplet MLCT state, which are in thermal equilibrium. This would result in a significantly weaker photoluminescence from the lower-energy state and a very low-emission intensity at helium temperatures.[20]

Examination of the emission data from the 11 compounds at room temperature and at 16 K and other considerations do not support this explanation. First, the energy gap between these states, reported as 1000−2000 cm^{-1},[13,19] would be too high compared with kT (∼210 cm^{-1} at room temperature) to allow establishment of a thermal equilibrium. Second,

(18) Basara, H. *J. Lumin.* **1983**, *28*, 73−86.
(19) (a) Kirchhoff, J. R.; Gamache, R. E.; Blaskie, M. W.; Del Paggio, A. A.; Lengel, R. K.; McMillin, D. R. *Inorg. Chem.* **1983**, *22*, 2380−2384. (b) Everly, R. M.; McMillin, D. R. *J. Phys. Chem.* **1991**, *95*, 9071−9075.
(20) (a) Dietrich-Buchecker, C. O.; Nierengarten, J. F.; Sauvage, J. P.; Armaroli, N.; Balzani, V.; De Cola, L. *J. Am. Chem. Soc.* **1993**, *115*, 11237−11244. (b) Armaroli, N.; Balzani, V.; Barigelletti, F.; De Cola, L.; Flamigni, L.; Sauvage, J. P.; Hemmert, C. *J. Am. Chem. Soc.* **1994**, *116*, 5211−5217.

Table 3. Solid State Absorption and Emission Data

|	BF$_4$ **1**	BF$_4$·0.5AC **2**	BF$_4$·0.5DMP **3**	PF$_6$ **4**	PF$_6$·CH$_2$Cl$_2$ **5**	NO$_3$·H$_2$O **6**	calix[4]arene **7**	*p*-Tos **8**	α-AQS **9**	β-AQS **10**	picrate **11**
					Reflectance (nm)						
	330	330sh	340sh	340sh	330sh	330sh	330sh	330sh	335sh	330sh	340
	420	415	426	410	404	432	403	418	428	420	425sh
	460sh	464sh	455sh	440sh	422sh	465sh	445	458sh	451sh	454sh	
	588	570	564	564	564	585	575sh	570	580sh	585	622
					Emission						
τ, μs (RT)	0.32	0.34	0.56	0.34	0.44	0.25	0.18	0.95	0.26	no emission	0.34
τ, μs (16 K)	0.76	0.80	1.3	0.50	0.95	0.11 0.44[a]	0.30	2.40	0.80	no emission	0.60
λ_{max}, nm (RT)	700	690	660	705	690	720	710	660	695	no emission	715
λ_{max}, nm (16 K)	720	710	705	710	720	730	750	690	730	no emission	760

[a] Biexponential fit to the emission decay curve.
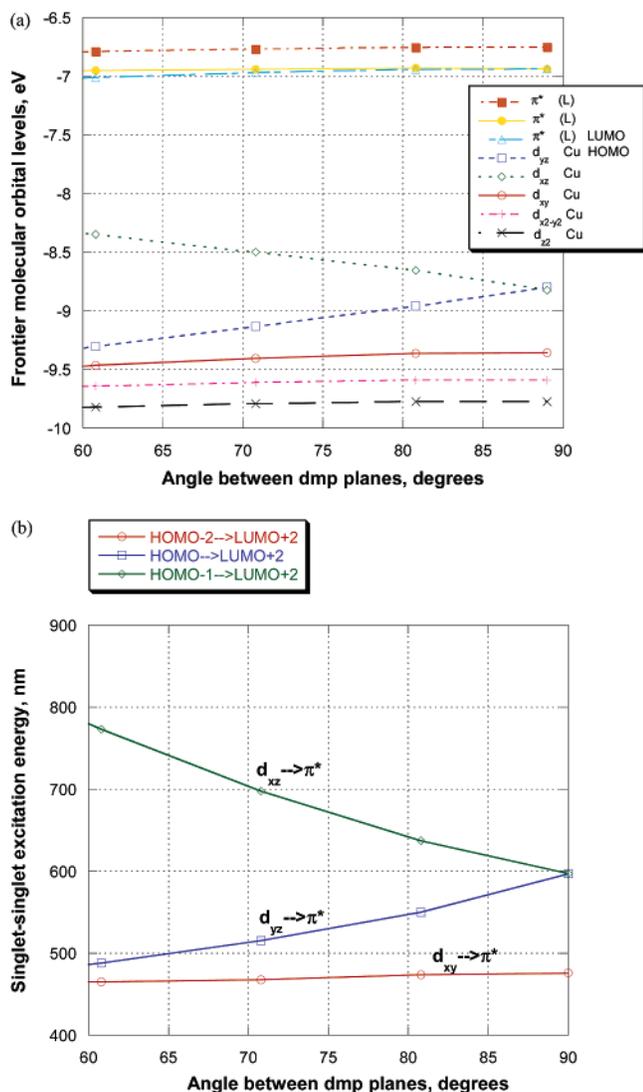
Figure 5. Top: Energy of the frontier orbitals of [Cu$^{(I)}$(dmp)$_2$]$^+$ as a function of the angle between the dmp planes. Bottom: Excitation energies from TD-DFT calculations.

unlike the data obtained by Shinozaki and Kaizu,[21] our emission decay curves could all be fitted adequately with a single-exponential decay, with the exception for compound **6**, for which the 16 K emission decay curve was fitted biexponentially. It is not impossible that the solid-state data

(21) Shinozaki, K.; Kaizu, Y. *Bull. Chem. Soc. Jpn.* **1994**, *67*, 2435−2439.

of Shinozaki and Kaizu are from multiphase samples, as the copper(I) complexes can occur in several polymorphic modifications, and/or cocrystallize with solvent molecules. Third, the reported room temperature excited state lifetimes are hundreds of nanoseconds, being longer than expected for fluorescence emission (Table 3), and the depicted pseudo-Stokes shifts are appreciable, as is typical for phosphorescence but not for fluorescence emission.

The lifetimes increase by a factor of 2−2.5 upon cooling the samples. The emission maxima move to lower energies, although the red-shifts are different for different compounds. For instance, for the PF$_6^-$ compound **4** the phosphorescence shifts merely 5 nm to the red on cooling, but for complexes **9** and **11** the shifts are 45 nm. Such shifts may be due to the contraction of the crystals, which will affect both the initial ground state and excited state energy levels. The temperature shift of the emission is just 100 cm^{-1} for complex **4**, but it increases to around 700 cm^{-1} for complexes **9** and **11**, while for the other compounds the values lie between these two extremes. When irradiated with 365 nm light, the emission intensity from crystals of the calixarenate (**7**) is so low that it could not be detected in our experiments. Interestingly, with 500 nm light illumination a very weak emission could be detected at both room and low temperatures.

The pronounced variation of the ^{3}MLCT excited state lifetime with the counterion is striking. It varies from 0.44 μs at 16 K for nitrate complex **6**, to 2.4 μs at 16 K for the tosylate compound, which is an increase of more than five times even though the ground state geometries of the Cu(dmp)$_2^+$ cations in these two solids are essentially identical, the π−π stacking interactions between the dmp ligands are weak in both compounds, and closest contacts with the neighboring counterions are comparable (Table 2). Thus, neither the ground state geometry nor the packing interactions in the crystalline phase appear to correlate with the photoluminescence properties of the complexes investigated. The extent of the cation's geometrical distortion upon photoexcitation to the triplet state remains as a possible source of the differences observed.

Emission Quenching in Anthraquinone Sulfonate Salts. Complexes **9** and **10** differ from the others studied here by having the electron accepting AQSO$_3$ as counterion, thus allowing the possibility of interionic charge transfer as a mechanism for phosphorescence quenching. Compounds **9**

and **10** are the first such copper(I) systems of which the structure and photoluminescent properties have been studied in the solid state. In previous studies of solutions of substituted bis-phenanthroline and bis(phosphine)phenanthroline copper(I) compounds,[5,22] it was shown that electron accepting molecules, such as substituted benzenes, anthracenes, viologens, and even small inorganic Co and Cr complexes, can easily quench the emission from a copper complex by either energy or electron transfer. The mechanism of the phosphorescence quenching was described as dynamic in nature. After excitation of the $Cu^{(I)}$ complex into its MLCT excited state, the excited molecule encounters the acceptor molecule, and the electron or energy is transferred during the lifetime of the encounter complex. The back reaction again occurs through such an encounter complex, without the copper molecule emitting light. However, in the solid state all the molecules are immobilized in the crystal matrix and subject only to the relatively small-amplitude vibrations and/or librations allowed by the crystal packing. Therefore, in the crystalline state the electron or energy transfer can happen only through space to neighboring molecules. For **10**, which is a crystalline hydrate with two independent Cu complexes in the asymmetric unit, no emission could be detected either at room or low temperature, indicating that the phosphorescence is largely quenched. However, in **9** (the α-form), the emission can be detected when the excitation wavelength is 500 nm (Table 3). A similar behavior was observed in the case of the picrate complex, which contains a weak acceptor ion. The fact that the two polymorphs have considerably different emissive properties points to the effect of the crystal packing on the luminescence properties. In the α-form, the $AQSO_3^-$ coun-

terion overlaps the nearest dmp ligand (Figure 4), though few close contacts occur, and only one 4.43 Å contact exists involving the copper atom. On the other hand, in the β-form (**10**), the $AQSO_3^-$ molecules form several contacts with both neighboring dmp ligands and with copper atoms (Table 2). In addition, each of the two copper atoms of the two symmetrically independent molecules has two close contacts of about 4.3−4.6 Å with oxygen atoms of the neighboring anthraquinone-sulfonate anions. Thus, the observed lack of luminescence of **10** may be due to the energy or electron transfer to the anion.

Conclusions

The comparison of a series of different solids all containing the $Cu(I)(dmp_2)^+$ ion shows a large variation in geometric distortion upon variation of the crystalline environment and a pronounced difference in spectroscopic properties. Red shifts of the longest wavelength absorption band are observed when the flattening exceeds 10° and the rocking distortion is less than about 5°. The 16 K phosphorescence lifetimes vary by a factor of about 5 between the different solids. In the anthraquinone salts, the phosphorescence is largely quenched, which is tentatively attributed to electron or energy transfer to the counterion. The lack of an obvious correlation between the ground state geometry differences among the complexes and the luminescence properties indicates the need for information on the excited state geometry as a function of the molecular environment. Such information can be obtained by time-resolved diffraction studies at atomic resolution, which are now becoming a reality.[1]

Supporting Information Available: Tables of crystallographic information. X-ray crystallographic files in CIF format for the structure of **1−11**. This material is available free of charge via the Internet at http://pubs.acs.org.

IC0348805

(22) (a) Sakaki, S.; Koga, G.; Ohkubo, K. *Inorg. Chem.* **1986**, *25*, 2330−2333. (b) Sakaki, S.; Koga, G.; Hinokuma, S.; Hashimoto, S.; Ohkubo, K. *Inorg. Chem.* **1987**, *26*, 1817−1819. (c) Crane, D. R.; Ford, P. C. *J. Am. Chem. Soc.* **1991**, *113*, 8510−8516. (d) Sakaki, S.; Mizutani, H.; Kase, Y.-I.; Arai, T.; Hamada, T. *Inorg. Chim. Acta* **1994**, *225*, 261−267. (e) Sakaki, S.; Mizutani, H.; Kase, Y.-I.; Inokuchi, K.-J.; Arai, T.; Hamada, T. *J. Chem. Soc., Dalton Trans.* **1996**, 1909−1914. (f) Ruthkosky, M.; Castellano, F. N.; Meyer, G. J. *Inorg. Chem.* **1996**, *35*, 6406−6412. (g) Ruthkosky, M.; Kelly, C. A.; Castellano, F. N.; Meyer, G. J. *Coord. Chem. Rev.* **1998**, *171*, 309−322.